ISCI, Volume 7

Supplemental Information

Glutamate Signaling in the Fly Visual System

Florian G. Richter, Sandra Fendl, Jürgen Haag, Michael S. Drews, and Alexander Borst

Supplemental Information

Supplemental Figures

A

L1	GCaMP6f	iGluSnFR
τ_{LP}	350 ms	70 ms
τ_{HP}	1178 ms	407 ms
$FWHM_{cen}$	8.74	10.56
$FWHM_{sur}$	56.55	42.55
A_{rel}	19.33	20.51

B

Mi9	GCaMP6f	iGluSnFR
τ_{LP}	607 ms	75 ms
$FWHM_{cen}$	6.69	7.18
$FWHM_{sur}$	19.37	25.86
A_{rel}	2.81	3.56

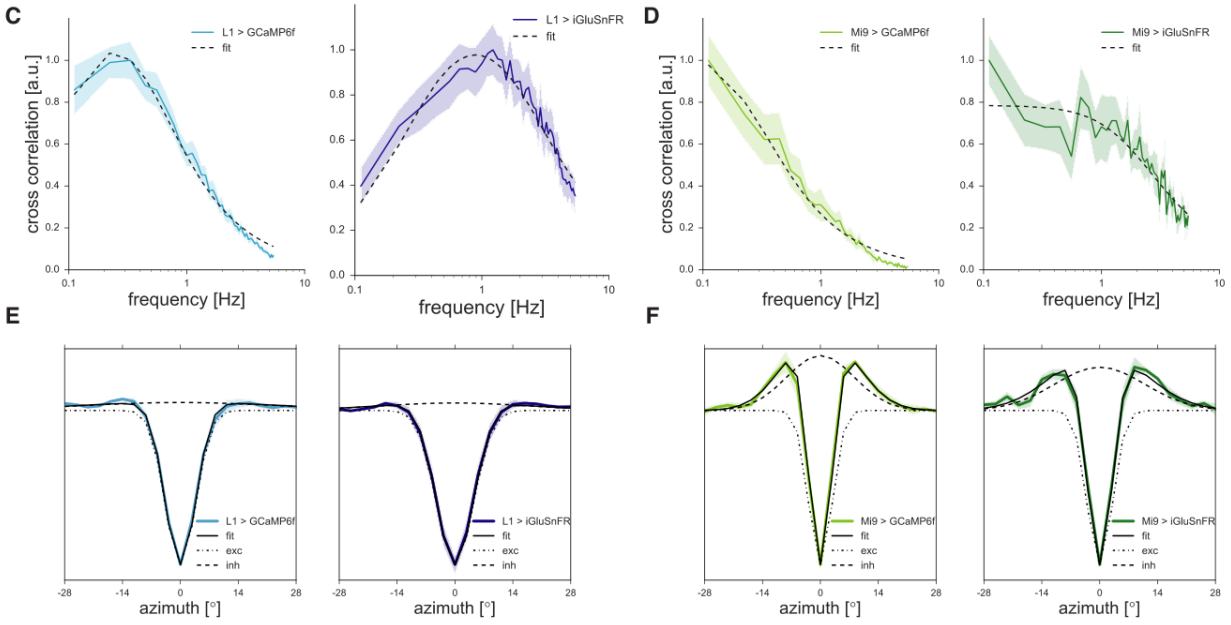

Figure S1. Model fits to L1 and Mi9 data, related to Fig 3
(A) Parameters to quantitatively describe the receptive field characteristics of L1 recorded either with GCaMP6f (left column) or iGluSnFR (right column). First two parameters describe temporal components of the receptive field, last three parameters describe those of the spatial component.
(B) Same as (A) only for Mi9. Description of highpass characteristics is missing, since Mi9 is best described by a pure low-pass.
(C) Impulse responses from Figure 3 D-E plotted in frequency space. Black dashed lines mark the fit of a 1st order band-pass filter (for time constants see table (A).
(D) Same as (C) only for Mi9. Black dashed lines mark the fit of a 1st order low-pass filter.
(E)+(F) Spatial receptive fields from Figure 3 D-E. Data are fitted with a Mexican hat function that captures both, the excitatory center as well as the inhibitory surround of these receptive fields. cen = center, sur = surround, LP = low-pass, HP = high-pass, A = amplitude, τ = time constant, FHWM = full width at half maximum.

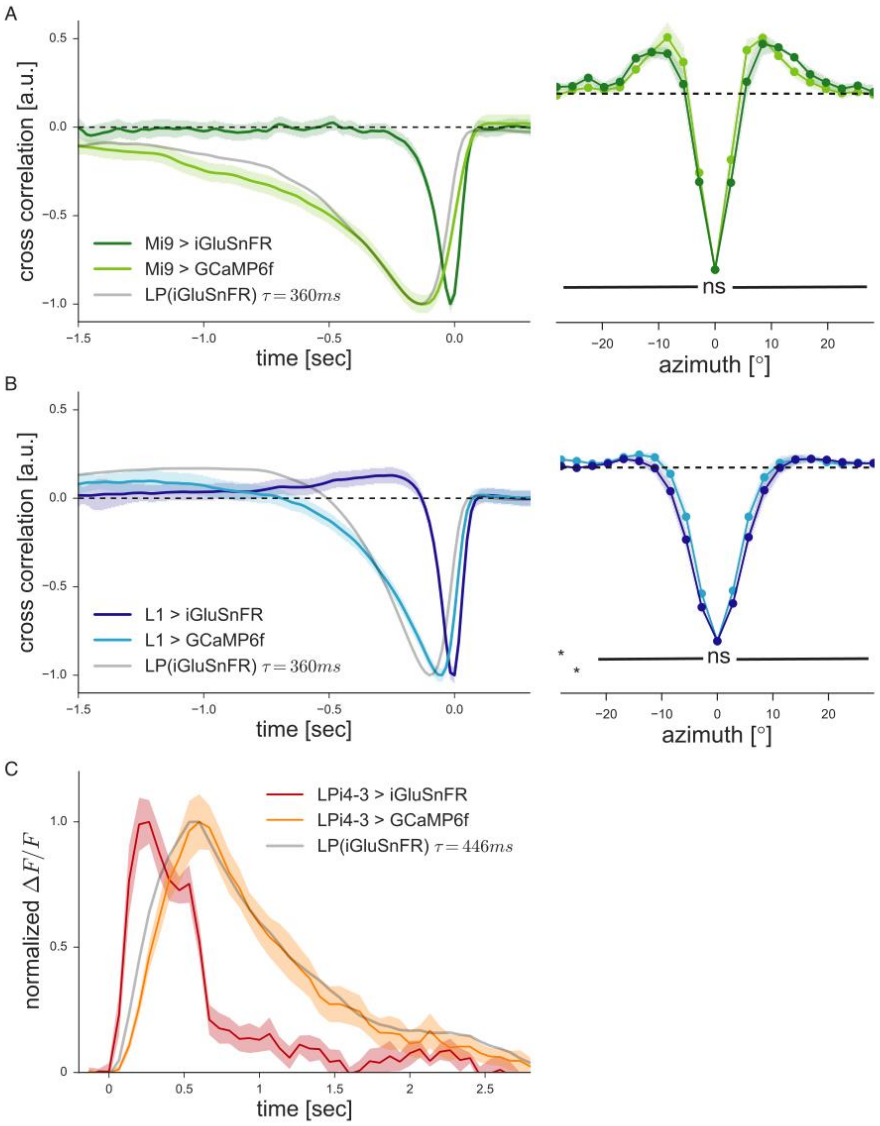

Figure S2. GCaMP data resembles low-pass filtered iGluSnFR data, related to Fig 3 and 4
(A) Low-pass filtering of the Mi9 impulse response measured with iGluSnFR with a time constant of 360 ms (grey) shows the best fit with the impulse response measured with GCaMP6f (left panel). Spatial receptive fields (right panel) are not significantly different from each other, when measured with the two different sensors.
(B) Same as (A) for L1
(C) Low-pass filtering of the LPi4-3 > iGluSnFR response to local flicker with a time constant of 446 ms (grey) shows the best fit to response measured with GCaMP6f (orange).

Transparent Methods

Flies/preparation

Flies were raised and kept on standard cornmeal-agar medium on a 12 hour light/12 hour dark cycle at 25°C and 60% humidity. For imaging experiments, the genetically-encoded calcium indicators GCaMP6f or the genetically encoded glutamate sensor iGluSnFR (Chen et al., 2013; Marvin et al., 2013) were expressed using the Gal4-UAS system in cell-type specific Gal4 fly lines, resulting in the following genotypes:

Genotypes:

L1>GC6f:	w+; R48A08-AD/UAS-GCaMP6f; R66A01-DBD/UAS-GCaMP6f
L1>iGluSnFR:	w+; R48A08-AD/+; R66A01-DBD/UAS-iGluSnFR (BL59611, AV184)
Mi9>GC6f:	w+; R48A07-AD/UAS-GCaMP6f; VT046779-DBD/UAS-GCaMP6f
Mi9>iGluSnFR:	w+; R48A07-AD/+; VT046779-DBD/UAS-iGluSnFR (BL59611, AV184)
LPi>GC6f:	w+; +/UAS-GCaMP6f; R38G02-Gal4/UAS-GCaMP6f
LPi>iGluSnFR:	w+; +; R38G02-Gal4/UAS-iGluSnFR (BL59611, AV184)

For immunohistochemical stainings in Figure 2:

L1>myr::GFP:	w-; R48A08-AD/UAS-myr::GFP; R66A01-DBD/+
Mi9>myr::GFP:	w-; R48A07-AD/ UAS-myr::GFP; VT046779-DBD/+
LPi4-3>myr::GFP:	w-; UAS-myr::GFP/+; R38G02-Gal4/+

The transgenic fly lines driving split-Gal4 expression in the lamina neuron L1 were generated and described in (Tuthill et al., 2013). Mi9 in (Strother et al., 2017) and the one of LPi's in (Mauss et al., 2015). For calcium and glutamate imaging experiments, flies were prepared as previously described (Maisak et al., 2013; Strother et al., 2017). Briefly, flies were anaesthetized on ice, fixed with their backs, legs and wings to a Plexiglas holder with the back of the head exposed to a recording chamber filled with fly external solution. The cuticle at the back of the head on one side was cut away with a fine hypodermic needle and removed together with muscles and air sacks covering the underlying optic lobe.

Data acquisition and analysis:

Data analysis was performed offline using custom-written routines in Matlab and Python 2.7 (with the SciPy and OpenCV-Python Libraries).

2-photon imaging:

Imaging was performed on custom-built 2-photon microscopes as previously described (Maisak et al., 2013) and controlled with the ScanImage software in Matlab (Pologruto et al., 2003). Acquisition rates were between 15 (for LPi experiments) and 23.67 Hz (for L1 and Mi9 experiments), image resolution between 64x64 and 128x32 pixels (for L1 and Mi9 experiments). Before starting the acquisition, we verified that the receptive fields of the cells were located on the stimulus arena by showing a search stimulus consisting of moving gratings.

Calcium imaging was performed as previously described in (Arenz et al., 2017). In brief: Images were automatically registered using horizontal and vertical translations to correct for the movement of the brain. Fluorescence changes (ΔF/F values) were then calculated using a standard baseline algorithm (Jia et al., 2011). Regions of interest (ROIs) were drawn on the average raw image by hand in the medulla layer M1 for L1 and in layer M10 for Mi9. For LPi neurons, ROIs were routinely chosen in the lobula plate, encompassing small regions with single to few axon terminals. Averaging the fluorescence change over this ROI in space resulted in a ΔF/F time course. Glutamate imaging was performed with the same settings as the calcium imaging experiments.

Visual stimulation for L1 and Mi9 experiments

The spatiotemporal response properties of the L1 and Mi9 columnar input elements were determined on a custom-built projector-based arena, as previously described in (Arenz et al., 2017). Stimuli were projected with 2 commercial micro-projectors (TI DLP Lightcrafter 3000) onto the back of an opaque cylindrical screen covering 180 ° in azimuth and 105 ° in elevation of the fly's visual field. The projectors refresh rate is 180 Hz (at 8 bit color depth). For all stimuli used here, we set the medium brightness to a 8-bit grayscale value of 50, which corresponds to a medium luminance of 55 ± 11 cd/m^2. Stimuli were rendered using a custom written software in Python 2.7.

Visual stimulation for LPi4-3 experiments with telescope

This technique has been previously described in (Haag et al., 2016). In brief: Antidromic illumination of the fly's head visualizes the hexagonal structure of the optical axes of the ommatidia (Franceschini, 1975; Schuling et al., 1989). Visual stimuli are generated on the AMOLED display (800x600 pixels, pixel size 15x15 mm, maximal luminance > 1500 cd/m^2; lambda = 530 nm; refresh rate 85 Hz) (SVGA050SG, Olightek). This allows to precisely position the stimuli onto single lamina cartriges. In order to prevent stimulus light from entering the photomultiplier of the two-photon micro-scope, light generated by the AMOLED display was filtered with a long-pass filter (514 LP, T: 529.4– 900 nm, AHF). The AMOLED display was controlled with MATLAB and the psychophysics toolbox (V3.0.11;(Brainard, 1997)).

White noise reverse-correlation

The analysis of spatial receptive fields was previously described in (Arenz et al., 2017). For the input elements, spatiotemporal receptive fields were calculated following standard reverse-correlation methods (Dayan and Abbott, 2013; French, 1976). First, the mean value was subtracted from the raw signals of single ROIs by using a low-pass filtered version of the signal (Gaussian filter with 120 seconds standard deviation) as a baseline for a ΔF/F-like representation of the signal.
The stimulus-response reverse correlation function was calculated as:

$$K(x,\tau) = \int_0^T dt\, S(x, t-\tau) \cdot R(t)$$

with S for the stimulus and R for the response of the neuron. The resulting spatiotemporal fields were normalized in z-score. Only receptive fields with peak amplitudes above 10 standard deviations from the mean were taken for further analysis (for Mi9-GCaMP6f the threshold

was lowered to 7). Cross-sections through the receptive fields along the space axis were fit with a Gaussian function to determine the position of the peak (Suppl. Fig. 1 E-F).

Gaussian noise stimulus

The same stimulus was used in (Arenz et al., 2017). In brief: The stimulus consisted of 64 vertical bars covering an angle of 180° in total. The intensity of each bar fluctuated randomly around a mean intensity of 50 on the 8-bit grayscale of the display. The intensities were drawn from a Gaussian distribution with a standard deviation of 25% contrast. In time, the stimulus was low-pass filtered with a Gaussian window with approximately 22ms standard deviation, which restricted the frequency content of the stimulus to frequencies below 10Hz. For Mi9-GCaMP6f imaging, similarly, the time window was 45ms long, covering frequencies until up to 5Hz.

Spatial receptive field

The analysis of spatial receptive fields was previously described in (Arenz et al., 2017). In brief: One-dimensional spatial receptive fields are cross-sections through the peak of the spatiotemporal receptive fields along the space axis and are averaged over the 12 samples (200ms) around the peak. For both L1 and Mi9 we found a small-field, antagonistic center-surround organization of the spatial receptive field using the vertical white noise stimulus.
The black dashed lines in Suppl. Fig 1 represents a Mexican hat function (Difference of Gaussian). Mathematically such a function can be described as follows:

$$RF_{1D}(\varphi) = e^{-\frac{1}{2}\frac{\varphi^2}{\sigma_{cen}{}^2}} - A_{rel} \cdot e^{-\frac{1}{2}\frac{\varphi^2}{\sigma_{sur}{}^2}}$$

with φ as azimuth, σ_{cen} and σ_{sur} as the standard deviations of center and surround, respectively, and $A_{rel} = A_{sur}/A_{cen}$ the relative strength of the surround in relation to the amplitude of the center Gaussian (which is normalized to 1).

Temporal receptive field

The analysis of temporal receptive fields was previously described in (Arenz et al., 2017). In brief: The time-reversed impulse responses shown in Figure 3 are cross-sections through the center of the spatiotemporal receptive fields along the time axis and are averaged over the three center pixels. For the determination of the time constants (tau), we sought to describe the response characteristic of each cell with a simplified model that catches the main properties. For that, we fitted simple 1st$_{st}$ order filters (e.g. 1st order low-pass for Mi9; 1st order bandpass for L1) to the impulse responses of all cells.
The model fit in Suppl. Fig 2 (grey lines) was performed by low-pass filtering the measured iGluSnFR response of each neuron type (L1, Mi9, LPi) with a 1st order low-pass filter and optimizing the time-constant such that the difference between the low-pass filtered signal and the measured calcium response of the neurons was minimal. The fitting procedure was implemented using standard least square algorithms (SciPy 0.19).

Immunohistochemistry

Fly brains were dissected in ice-cold 0.3% PBST and fixed in 4% PFA in 0.3% PBST for 25 min at room temperature. Subsequently, brains were washed 4-5 times in 0.3% PBST and blocked in 10% normal goat serum (NGS) in 0.3% PBST for 1 hour at room temperature. Primary antibodies used were mouse anti-bruchpilot brp (nc82, Developmental Studies

Hybridoma Bank, 1:20) and rabbit anti-VGlut (courtesy of H. Aberle, 1:500). Secondary antibodies used were: goat anti-mouse ATTO 647N (Rockland, 1:300) and goat anti-rabbit Alexa Fluor 568 (Life Technologies, 1:300). Myr::GFP-labeled cells were imaged natively without antibody staining. 5% NGS was added to all antibody solutions and both primary and secondary antibodies were incubated for at least 48 hours at 4°C.
Brains were mounted in Vectashield Antifade Mounting Medium (Vector Laboratories) and imaged on a Leica TCS SP8 confocal microscope.

Supplemental References

Brainard, D.H. (1997). The psychophysics toolbox. Spat. Vis. 10, 433–436.

Franceschini, N. (1975). Sampling of the visual environment by the compound eye of the fly: Fundamentals and applications. Photoreceptor Opt. 98–125.

Jia, H., Rochefort, N.L., Chen, X., Konnerth, A. (2011). In vivo two-photon imaging of sensory-evoked dendritic calcium signals in cortical neurons. Nat. Protoc. 6, 28–35.

Pologruto, T.A., Sabatini, B.L., Svoboda, K. (2003). ScanImage: Flexible software for operating laser scanning microscopes. Biomed. Eng. Online 2.

Schuling, F.H., Mastebroek, H.A.K., Bult, R., Lenting, B.P.M. (1989). Properties of elementary movement detectors in the fly *Calliphora erythrocephala*. J. Comp. Physiol. A 165, 179–192.